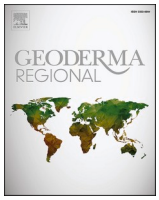
Geoderma Regional 42 (2025) e00987



Contents lists available at ScienceDirect

Geoderma Regional

journal homepage: www.elsevier.com/locate/geodrs



Controls on soil respiration in alpine tundra

Sarah A. Schliemann [a,*], Nels Grevstad [b], David A. Parr [c]

[a] Metropolitan State University of Denver, Earth and Atmospheric Science, Science 2028, 1150 12th St., Denver, CO 80217, United States of America
[b] Metropolitan State University of Denver, Department of Mathematics and Statistics, Science 1030, 1150 12th St., Denver, CO 80217, United States of America
[c] The University of North Carolina at Chapel Hill, Department of Geography and the Environment, UNC Department of Geography and Environment, 220 E. Cameron Avenue, 205 Carolina Hall, Chapel Hill, NC 27599-3220, United States of America

ARTICLE INFO

Keywords:
Soil respiration
Alpine tundra
Climate change
Soil organic carbon (SOC)
Southern Rocky Mountains
Inceptisols

ABSTRACT

Alpine tundra ecosystems, like their arctic counterparts, have historically been the sites of considerable soil organic carbon (SOC) storage due to climatic factors that suppressed microbial activity. While climatic factors are important, heterotopic soil respiration (and SOC storage) may be influenced by a range of soil characteristics. In this study, we measured soil respiration, soil temperature, soil moisture, soil nutrient concentrations, soil pH, and soil texture in 4 alpine tundra sites located in Rocky Mountain National Park, Colorado, USA from June 2015 – September 2021. We also used geospatial modeling to visualize predicted climate changes in this system over the 21st century. Finally, we measured SOC concentrations over the seven-year study. We found that soil respiration was significantly correlated with soil temperature, soil moisture, and soil texture. All other parameters were not significantly correlated with soil respiration. We also found that SOC concentrations did not change significantly over the course of the seven-year study. The predictive models show that by the end of the century, over the majority of the park, the mean maximum air temperature will increase, the amount of snowfall will decrease, soil moisture will decrease, and the number of snow-free days will increase. These results suggest that SOC is not currently being lost from this system at a high rate. In addition, it appears that with a changing climate, soil respiration may increase with warming, but the overall increase may be limited by decreased soil moisture and in some cases, high soil temperatures.

1. Introduction

Alpine tundra ecosystems, like their arctic counterparts, have historically been the sites of considerable soil organic carbon (SOC) storage due to climatic factors that suppressed microbial activity (Schuur et al., 2008; Turetsky et al., 2020; Wu et al., 2021). Although all cold-climate areas have the potential to hold significant SOC, permafrost represents the largest pool of terrestrial carbon (C), accounting for more than 65 % of all non-fossil C on land in 2022 (Friedlingstein et al., 2022). Permafrost is found in areas in which the soil remains below freezing for two or more consecutive years. These areas are primarily located in high latitude regions but are also found at high elevations at lower latitudes, even into the tropics (Gruber, 2012).

Globally, alpine tundra soils with permafrost contain 66.3 Pg of organic C, which constitutes 4.5 % of the global SOC pool (Bockheim and Munroe, 2014). In the Southern Rocky Mountains, there are some isolated, discontinuous patches of permafrost located in higher elevations with cool microclimates, but today much of the area is too warm to support permafrost. Thus, the carbon-storage capacity of this region may have been altered over the last several decades (Janke, 2005; Knowles et al., 2019). Rocky Mountain alpine soils have been found to contain 0.12–17.22 % of SOC within the top 15 cm (Birkeland et al., 1987; Retzer, 1974). It is often assumed that as temperatures continue to rise, SOC losses will accelerate, especially in cold-climate soils, such as those at high elevations.

According to the IPCC's Sixth Assessment Report, global temperatures have warmed 1.09 °C since 1850–1900 and will reach 1.5 °C warming within the next 20 years (Lee and Romero, 2023). This warming is expected to continue. CMIP6 modeling projects a warming of 2.5–6.1 °C globally by the end of the century (Gutiérrez et al., 2021; Tebaldi et al., 2021). On a local scale within our study area, warming has also been observed. Within Rocky Mountain National Park, winter air temperatures warmed by 0.29C per decade from 1981 to 2015 (Fassnacht et al., 2018).

Historical data and model predictions show that warming is often more pronounced in mountainous regions. Elevation-dependent

* Corresponding author.
E-mail address: sschliem@msudenver.edu (S.A. Schliemann).

https://doi.org/10.1016/j.geodrs.2025.e00987
Received 6 April 2025; Received in revised form 3 July 2025; Accepted 13 July 2025
Available online 14 July 2025
2352-0094/© 2025 Elsevier B.V. All rights are reserved, including those for text and data mining, AI training, and similar technologies.

warming (EDW) is driven by a range of factors including water vapor changes and latent heat release, aerosol loading, water vapor-radiative feedbacks, and the snow albedo feedback in which an increase in snow-free days results in a decrease in albedo and a corresponding increase in temperature (Auer et al., 2007; Pepin et al., 2015). Using high-resolution regional climate models, researchers have found similar enhanced warming at higher elevations in the Southern Rocky Mountain Region (Mahony et al., 2022; Minder et al., 2018).

In mountainous regions, climate change is not only altering temperature, but also precipitation type and soil moisture. Warming temperatures are leading to a reduction in snow cover duration, with precipitation coming as rain later in the fall and earlier in the spring. As temperatures rise, snowmelt is occurring earlier and evapotranspiration rates are increasing, which is leading to late summer soil dryness (Almazroui et al., 2021; Dethier et al., 2022; Dong et al., 2019; Fassnacht et al., 2018; Rasmussen et al., 2014).

SOC decomposition and C loss, is mediated by microbes and is influenced by a range of parameters including soil temperature, soil moisture, nutrient availability, soil pH, soil texture, and the magnitude and chemical characteristics of organic C input into the system (Davidson and Janssens, 2006; Giesler et al., 2012; Guo et al., 2022; Liu et al., 2009; Moyano et al., 2012). It is generally thought that microbial decomposition of SOC is controlled most strongly by soil temperature and soil moisture. With an increase in soil temperature, there is generally an increase in microbial activity and soil respiration (SOC loss) (Davidson and Janssens, 2006; Lloyd and Taylor, 1994; Xue et al., 2016; Zhou et al., 2019), although if the optimum soil temperature is surpassed, the rates will decrease (Alster et al., 2022; Liu et al., 2018). Soil respiration also tends to be positively related to soil moisture, but at very high levels of soil moisture, rates of soil respiration may also slow (Davidson et al., 1998; Liu et al., 2009; Moyano et al., 2013).

Soil texture, in particular clay content, may also influence soil respiration through its effect on soil moisture. At lower levels of soil moisture, clay content appears to enhance soil respiration while at high levels of soil moisture, it restricts soil respiration (Moyano et al., 2012; Xu et al., 2016). Thus, the role of soil texture in soil respiration may vary over the course of the year and from location to location as soil moisture varies.

Nutrient availability, especially nitrogen (N) and phosphorus (P), may also influence soil respiration. In some soils with significant labile C, N additions can result in increased microbial growth (Wardle, 1992) and an increase in soil respiration. However, in most natural systems, soils with high N concentrations in any inorganic form, tend to have lower levels of soil respiration and are instead associated with C sequestration (Craine et al., 2007; Guo et al., 2022; Janssens et al., 2010; Shahbaz et al., 2022; Treseder, 2008). High N additions are associated with a decrease in pH, which may limit microbial growth and heterotrophic soil respiration (Song et al., 2019). In addition, under high N conditions, plants tend to allocate more C to above ground structures and limit below ground allocation which may result in a reduction in mycorrhizal fungi growth and SOC accumulation. N availability could also result in changes in the overall microbial community structure, which could result in a reduction in heterotrophic respiration (Janssens et al., 2010).

In contrast to N, P appears to have a less direct effect on SOC decomposition. Giesler et al. (2012) found that P availability influenced soil microbial function in a tundra ecosystem, but the effect was reasonably small. In their study on the Qinghai-Tibetan Plateau, Ren et al. (2016) found that P availability influenced autotrophic soil respiration but not heterotrophic soil respiration. An increase in autotropic soil respiration would likely result in an increase in SOC, which could possibly contribute to elevated rates of heterotrophic soil respiration due to an increase in substrate (C) availability.

Soil pH influences a range of abiotic factors including organic C (SOC) and nutrient availability (Kemmitt et al., 2006) and soil microbial community composition (Song et al., 2019). Fungal growth is greatest under lower pH conditions and bacterial growth is greatest at higher pH. In general, it appears that soil respiration is positively correlated with pH, although only for pH values between 5 and 8.5. Values outside this range tend to suppress soil respiration (Guo et al., 2022; Leifeld et al., 2008; Rousk et al., 2009).

In this project, we had several objectives. First, we set out to determine which of the known drivers of soil respiration (e.g. soil temperature, soil moisture, soil texture, soil N concentration, soil P concentration, and soil active and exchangeable pH) were the strongest predictors of soil respiration in the alpine tundra system. Second, using our data on drivers of soil respiration, we used climate models to make predictions about future soil respiration in the Southern Rocky Mountains. Third, we measured SOC concentrations over the course of the study to determine whether soil carbon concentrations were changing in this alpine tundra system.

2. Materials and methods

2.1. Field methods

In June of 2015, we established two 225 m^2 alpine tundra study sites in Rocky Mountain National Park, Colorado, USA (Fig. 1). Site 1 was a wet meadow, located in the saddle between two hills, at 3684 m in elevation (m above sea level). It was characterized by relatively deep (30–40 cm) mineral soil and the presence of water through mid-summer in numerous small depressions. The vegetation mainly consisted of grasses, sedges, and hydrophytic forbs. Site 2 was a fellfield, located at the top of a hill exposed to near-constant wind at 3682 m in elevation. The area had very shallow (5–15 cm), rocky soil. During our study, vegetation covered less than 50 % of site 2 and was predominantly low-stature forbs.

In the summer of 2017, two additional meadow tundra sites were added (sites 3 and 4) (Fig. 1). Site 3 was located at 3691 m in elevation. The area was located near the top of a hill and was subjected to near-constant wind. The soil was very rocky, but more developed (10–20 cm deep) than the soil of site 2. The vegetation consisted of grasses and forbs. Site 4 was located at 3650 m in elevation at the foot of a large hill and was relatively sheltered from the wind. The soil was the deepest (> 40 cm) of all four sites and remained moist for much of the summer. The vegetation was similar to that of site 3 and consisted of grasses and forbs. Soils in all four sites are part of the Trailridge and Mummy series. Soils in these series are Typic Humicryepts (Soil Survey Staff, 2025).

Within each site, 2 20 cm PVC collars were installed to establish permanent sampling locations for measuring soil respiration. Data were collected from June 2015 – September 2021. Soil respiration was measured every two weeks during the snow-free period (June – September) using a Li-Cor LI-8100 A automated CO_2 flux system (Li-Cor, 2025). On each sampling date, the Li-Cor collected 5 replicate measurements in succession at each collar; total measurement time was ~20 min per collar. In addition, soil temperature and soil moisture were measured once within 20 cm of the soil respiration collar. To measure soil moisture and temperature, 15 cm probes were inserted perpendicular to the soil surface to a depth of 15 cm and soil temperature and soil moisture were measured along the length of the probe, from the soil surface to a depth of 15 cm. Soil temperature was measured using a digital soil probe thermometer with an accuracy of ±1.5 °C (Thomas Scientific, 2025). Soil moisture was measured using a Campbell Scientific HydroSense II probe, which uses dielectric permittivity to measure volumetric water content, with an accuracy of ±0.05 % (Campbell Scientific, 2025).

2.2. Laboratory analysis

Once a month, soil was collected from 6 randomly selected locations within each site using a 2.54 cm diameter soil corer to a depth of 15 cm. In the lab, each soil specimen was homogenized using a 4 mm sieve and

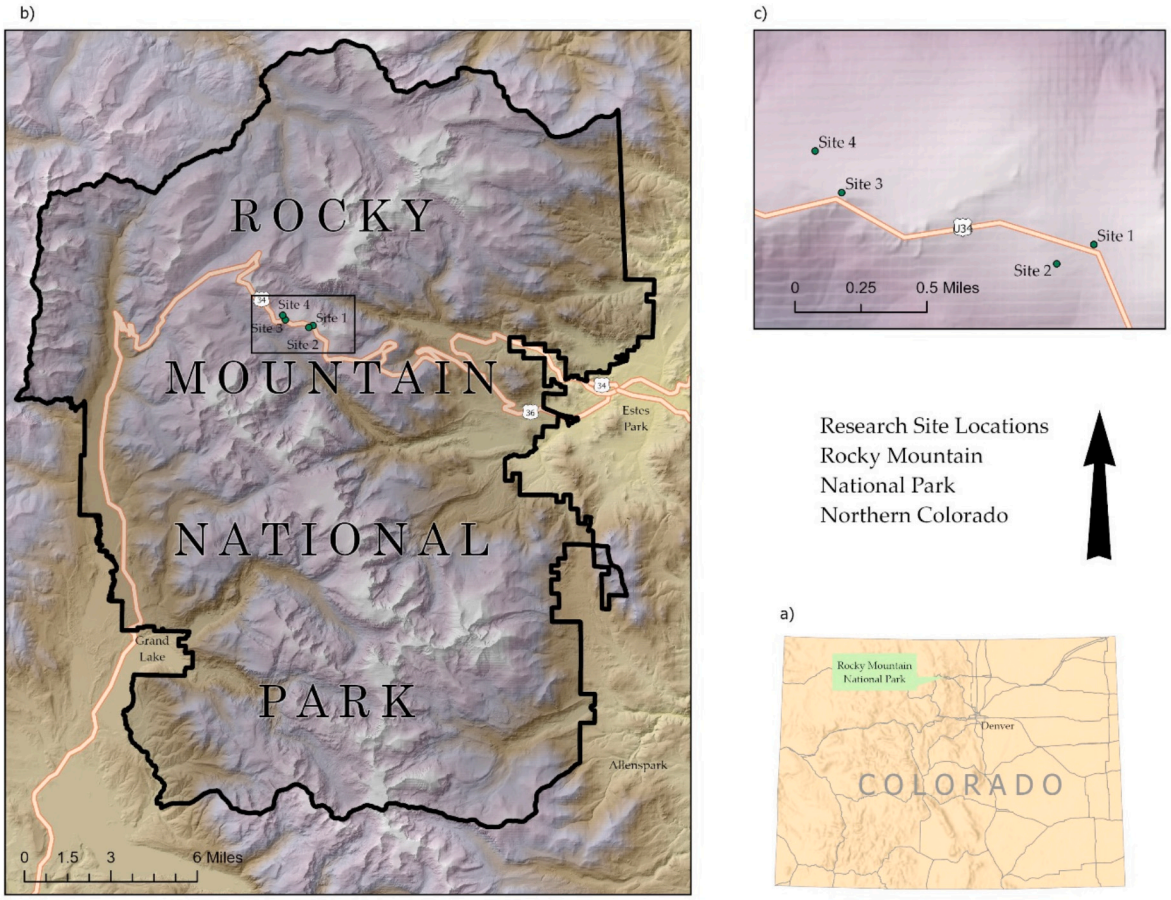


Fig. 1. Study location in Rocky Mountain National Park, Colorado, USA. The location of the park within the state of Colorado is shown in a), the location of the sites within the park is shown in b), and a detailed view of the sites is shown in c).

a sub-sample was extracted using a 2 M KCl solution. Ammonium- nitrogen (NH_4^+-N) was measured using a modified indophenol blue method (Sims et al., 1995) and read at 650 nm on a BioTek Gen5 microplate reader (Agilent, 2025). Phosphate- phosphorus (PO_4^{3-}-P)was measured using a modified malachite green method using a Malachite Green Phosphate Assay Kit from Sigma-Aldrich (Sigma Aldrich, 2025) and read on a BioTek Gen5 microplate reader at 650 nm (Agilent, 2025).

We used Hach Ag/AgCl gel-filled pH probes with a resolution of 0.01 to assess active and exchangeable soil pH using a 1:1 soil water solution (active pH) and a 1:1 2 M KCl solution (exchangeable pH). The probe was calibrated daily according to manufacturer instructions using a three-point standard calibration curve (Hach CO, 2025).

SOC concentration was assessed using a solid soil combustion method using a Shimadzu SSM-5000 A Total Carbon Analyzer (Shimadzu, 2025). Samples were dried and ground to <75 μm in size using a mortar and pestle before analysis. A standard curve was established using varying masses of dextrose according to manufacture instructions. Soil texture (sand, silt, and clay percentages) was determined using the hydrometer method (Gee and Bauder, 1986).

2.3. Statistical analysis

For each sampling date and each site, the soil respiration (CO_2 flux), soil temperature, soil moisture, and each set of soil parameter values were averaged, to obtain a single observation of each of these variables on each date at each site. This led to an overall sample size of $n = 168$ (multivariate) observations of CO_2 flux, soil moisture, and soil temperature. Of these, 76 also included measurements of soil nutrient and pH parameters.

To evaluate the relationship between CO_2 flux and the soil variables PO_4^{3-}-P, organic C (SOC), and NH_4^+-N, we fitted the multiple regression model.

$$\text{Flux}_{ijk} = \text{Site}_i + \text{Month}_j + \text{Year}_k + \beta_1 \times {PO_4}^{3-} - \text{P} + \beta_2 \times \text{Organic C} + \beta_3 \times {NH_4}^+ - \text{N} + \beta_4 \times \text{pH} + \varepsilon \quad (1)$$

Flux_{ijk} is the CO_2 flux at Site i, during Month j, in Year k. Site_i ($i = 1, 2, 3, 4$) is a categorical variable (with 4 levels corresponding to study sites) that controls for extraneous factors that may differ across sites such as unmeasured soil characteristics, amounts of sunlight, etc. Month_j ($j = 1, 2, \ldots, 4$) is a categorical variable (with 4 levels corresponding to June, July, August, and September) that is used to statistically test for a seasonal effect on CO_2 flux. Year_k ($k = 1, 2, \ldots, 7$) is a categorical variable (with 7 levels corresponding to the years 2015–2021) and is used to statistically test for yearly changes in CO_2 flux levels over the duration of the study. PO_4^{3-}-P, Organic C (SOC), and NH_4^+-N are the values of those soil variables associated with the CO_2 flux observation, pH is the active soil pH or exchangeable pH, and ε is a random error term assumed to follow a normal distribution that is homoscedastic (i.e. whose standard deviation does not change with the explanatory variables in the model).

To evaluate the relationship between CO_2 flux and the soil texture variables (percent clay, percent silt, and percent sand), we first fitted the model.

$$\text{Flux}_{ijk} = \text{Month}_j + \text{Year}_k + \beta_1 \times \text{Clay}_i + \varepsilon \quad (2)$$

where Flux_{ijk}, Month_j, Year_k, and ε are as defined previously, and Clay_i is the percent clay in the soil at Site i. Then separately, we fitted the same model but with percent Sand replacing Clay. Finally, we fitted the same

model but with percent Silt replacing Clay. The three models were fitted separately (rather than fitting a single model including Sand, Silt, and Clay) to alleviate problems due to multicollinearity. Site was omitted from these models because Site was confounded with Sand, Silt, and Clay (the texture did not fluctuate over visitation dates like the other soil variables did).

To investigate the relationship between CO_2 flux and the two explanatory variables soil temperature and soil moisture, we first fitted the full multiple regression model.

$$\begin{aligned}\text{Flux}_{ijk} = \text{Site}_i + \text{Month}_j + \text{Year}_k + \beta_1 \times \text{Temp} + \beta_2 \times \text{Moist} \\ + \beta_3 \times \text{Temp}^2 + \beta_4 \times \text{Moist}^2 + \beta_5 \times \text{Temp} : \text{Moist} + \varepsilon \end{aligned} \quad (3)$$

where Flux_{ijk}, Site_i, Month_j, Year_k, and ε are as defined previously. Temp and Moist are the soil temperature and soil moisture associated with the CO_2 flux observation. Their quadratic terms are included so CO_2 flux isn't constrained to follow a strict linear relationship to soil temperature and soil moisture, but instead can rise and then fall again as these variables become too high. Both soil temperature and soil moisture were centered (by subtracting the mean from each observation) prior to model fitting, as is commonly done in quadratic regression analyses, to alleviate multicollinearity (Kutner et al., 2004). Temp:Moist is the interaction effect between soil temperature and soil moisture, and it allows for the possibility that the effect of either of these variables may be different depending on the level of the other one.

Finally, to investigate whether organic C (SOC) was changing over time, we fitted the model

$$\text{Organic C}_{ijk} = \text{Site}_i + \text{Month}_j + \text{Year}_k + \varepsilon \quad (4)$$

where Organic C_{ijk}, is the organic C (SOC) at Site i, during Month j, in Year k, and Site_i, Month_j, Year_k, and ε are as defined previously. The statistical significance of the Year_k term in this model is of interest because it indicates whether organic C (SOC) changed over the study years.

Observations made close together in space and time are often correlated. To account for this spatio-temporal correlation, we fitted the models using generalized least squares (GLS), which allows for correlated observations, with a Gaussian spatio-temporal correlation structure (Wikle et al., 2019). This says the correlation between two CO_2 flux observations Y_a and Y_b a spatio-temporal distance d^{st} apart in space and time is

$$cor(Y_a, Y_b) = e^{-\left(d^{st}/r\right)^2}, \quad (5)$$

where the range parameter r controls the spatio-temporal extent of the correlation. A larger r value means the correlation extends farther (decays more slowly) over space and time. As mentioned in Wikle et al. (2019), we need to appropriately scale time to make Euclidean distance across space and time meaningful. Denoting the scaling factor by τ, following Liu et al. (2017) the spatio-temporal distance d^{st} between a location s_a on day t_a and another location s_b on a different day t_b is a combination of the spatial distance d^s (meters) and temporal distance d^t (days),

$$d^{st} = \sqrt{\left(d^s\right)^2 + \left(\tau \times d^t\right)^2} \quad (6)$$

where τ is the time-scaling factor that balances the different scales of spatial and temporal distances. If τ was equal to 1, the correlation between two CO_2 flux values one meter apart (on the same day) would be the same as the correlation between two CO_2 flux values one day apart (at the same location). For larger values of τ, the correlation between two CO_2 flux values one meter apart would be the same as the correlation between two CO_2 flux values less than one day apart. We selected the values of r and τ using maximum likelihood and fitted the models to the data in R using the "nlme" package (Pinheiro et al., 2025).

In addition to fitting the full model (3), we fitted submodels obtained by dropping one or more of the soil temperature and soil moisture terms from the full model (but retaining the site, month, and year terms). We evaluated the adequacy of the fitted models using the Akaike Information Criterion (AIC), a widely used statistical measure of the (relative) quality of different models, and the (pseudo) R-squared measure of Nagelkerke, which, unlike the standard R-squared, can be used with GLS models. Models with lower AIC values and ones with higher (pseudo) R-squared values are deemed better suited for explaining CO_2 flux variation.

Statistical significance of all model terms was assessed using regression t-tests at the 0.05 significance level. We checked the normality and homoscedasticity assumptions for the error term ε via plots of residuals.

2.4. Geospatial analysis

To evaluate the larger impacts of predicted climatic changes in Rocky Mountain National Park and the Southern Rocky Mountains, four variables were selected for mapping – Snow Water Equivalence (Snowfall), Soil Water Storage, Daily Maximum Air Temperature, and the number of Snow-Free Days within one year. Snowfall in Rocky Mountain National Park is critical for the high-mountain habitat in the park and meltwater from the snowpack constitutes the headwaters for various rivers including the Colorado River. Soil water storage (soil moisture) is critical for plant growth and productivity. Daily Maximum Air Temperature values indicate how quickly snow may melt. Snow-free Days indicate how much of the year areas will be clear of snow.

Downscaled data from the Northern Rocky Mountain Science Center and the Northwest Climate Science Center that included predictions for the 2090–2099 time frame were pulled (Table 1). Python and Jupyter Notebook were used to extract and collate data. For the first three variables (Snow Water Equivalent, Soil Water Storage, and Daily Maximum Air Temperature), historically computed values between 1950-and 1999 were compared with prediction values in the decade 2090–2099. The last variable, Snow-free Days, compares the pre-industrial predictions for snow-free days with climate change predictions during the 2071–2100 time period. Where possible, data with the finest resolution designated in the northern Colorado area was chosen.

3. Results

3.1. Statistical results

Site 1 had the highest mean soil respiration rate, soil moisture, NH_4^+-N concentration, and SOC concentration. Site 2 had the lowest soil

Table 1
Data used for geospatial analysis, including the model, dataset(s) and spatial resolution for each parameter.

Variable	Model	Dataset(s)	Spatial Resolution
Snowfall as Snow Water Equivalent (mm)	CMPI5, MACAv2, RCP8.5	1950–2005, 2006–2099. Northern Rocky Mountain Science Center (Alder and Hostetler, 2021).	4 km
Soil Water Storage (%)	CMPI5, MACAv2, RCP8.5	1950–2005, 2006–2099. Northern Rocky Mountain Science Center (Alder and Hostetler, 2021).	4 km
Daily Maximum Air Temperature (Celsius)	CMIP5, MACAv2, RCP4.5	1950–2005, 2006–2099. Northwest Climate Science Center (Abatzoglou, 2014).	4 km
Snow-Free Days	CMIP5, RCP8.5	PRE and PGW SnowClim v1.0 High-resolution snow model for the western United States. Northwest Climate Science Center (Abatzoglou et al., 2022).	210 m

moisture, PO_4^{3-}-P, NH_4^+-N, and SOC. Site 3 had the lowest mean soil respiration rate and the highest mean soil temperature, active soil pH, and exchangeable soil pH. Site 3 was also the only loam; the other sites were sandy loams (Table 2).

The model (1) fitted to PO_4^{3-}-P, organic C (SOC), NH_4^+-N, and active or exchangeable pH did not result in any statistically significant associations between these variables and CO_2 flux ($p > 0.05$). However, the model (2) fitted separately to percent clay and percent sand revealed CO_2 flux had a statistically significant positive relationship to clay and a statistically significant negative relationship to sand ($p < 0.05$). Percent silt was not significant ($p > 0.05$).

The models that were fitted to the soil temperature and soil moisture data are listed in Table 3 along with their AIC and (pseudo) R-squared values. The fitted full model (3) (M13 in Table 3) is shown in Fig. 2. Plots of CO_2 flux separately versus soil temperature and soil moisture, with fitted quadratic models (M5 and M6, respectively, in Table 3), are shown in Figs. 3 and 4. Four models stood out as superior based on their low AIC values. All four standout models had AIC values within about 2 of each other, implying they can be considered equally adequate for explaining CO_2 flux variation (Burnham and Anderson, 2002).

All four lowest-AIC models (M7, M10, M11, and M13 in Table 3) included soil moisture and both a linear and a quadratic soil temperature term, and in all four models these terms were statistically significantly related to CO_2 flux. The importance of the quadratic soil temperature term may be due to just a few low CO_2 flux observations at relatively high soil temperatures (Figs. 2 and 3). Two of the models (M10 and M13) also included a quadratic soil moisture term, and two (M11 and M13) included an interaction effect between soil temperature and soil moisture. Thus, it's clear that CO_2 flux is related to both soil temperature and soil moisture, and it may exhibit a quadratic relationship to soil temperature. Furthermore, there are indications that CO_2 flux may also exhibit a mild quadratic relationship to soil moisture too, and that the effect of soil moisture on CO_2 flux may differ slightly depending on the soil temperature, and vice versa.

Although CO_2 flux was found to change statistically significantly across years in all four lowest-AIC models, the pattern of change was not a steady increase over the years, but rather a drop in 2020 followed by a rise in 2021.

The model (4) used to assess changes in organic C (SOC) over the study years did not reveal any statistically significant change in organic C over the years.

Plots of the residuals indicated that the normality and homoscedasticity assumptions for the errors ε were met for all models.

Our soil temperature readings indicate that none of our sites contained permafrost within the upper 15 cm, as we recorded above-freezing temperatures at all locations on a yearly basis (Table 2).

3.2. Geospatial analysis results

Using the climate prediction data, it appears that by the end of the century, the average daily maximum air temperature will increase by 3–3.5 °C for all locations within Rocky Mountain National Park (Fig. 5). In addition, nearly all locations within the park will receive less snowfall on an annual basis, with a decrease of over 200 mm for about half the area (Fig. 6). Many areas in the park will also have more snow-free days per year (Fig. 7). Finally, soil moisture will decrease in all areas within the park (Fig. 8).

4. Discussion

Heterotrophic soil respiration is driven by soil microbial activity which can be influenced by a range of parameters, including soil temperature, soil moisture, nutrient availability, soil texture, and soil pH (Davidson and Janssens, 2006; Giesler et al., 2012; Guo et al., 2022; Liu et al., 2009; Moyano et al., 2012). However, in this investigation, we found that through the snow-free period, soil temperature, soil moisture, and soil texture were the only variables correlated with soil respiration.

Considering the four best fit models (M7, M10, M11, M13 in Table 3), it appears that the relationship between soil respiration and soil temperature and soil respiration and soil moisture in this system may be quadratic and there may be an interaction between soil temperature and soil moisture.

In this study, soil respiration was suppressed at high and low soil temperatures (Fig. 3). Our highest soil temperature readings, over 15 °C, were observed at site 2, which is a south-facing fellfield site, and site 3, a meadow. While 15 °C is not generally considered exceptionally high, in the alpine tundra, it may represent a sufficient deviation from the norm to suppress soil respiration. Soil temperature measurements over 15 °C represented less than 2 % of all observed soil temperatures and were relatively rare. The mean soil temperature measured during the snow-free period across all sites and study years was 6.8 °C. Others have observed lower heterotrophic respiration at high soil temperatures (Carey et al., 2016; Pietikainen et al., 2005). Carey et al. (2016) hypothesized that at higher soil temperatures, there was a decrease in microbial enzymatic activities due to physiological limitations due to heat.

While many studies have found a positive relationship between soil respiration and soil moisture (Liu et al., 2009; Orchard and Cook, 1983; Smith, 2005), it appears that in some cases, soils with exceptionally high soil moisture contents may display limited soil respiration. Knowles et al. (2015) found that in wet alpine tundra systems, soil respiration was limited when soil moisture increased beyond a threshold point of 38 %. The authors theorize that respiration was suppressed at high soil moisture values due to oxygen limitations. Similarly, Sun et al. (2021) found wet meadows with shallow groundwater and nearly saturated

Table 2
Summary statistics for CO_2 flux (soil respiration), soil temperature, soil moisture, PO_4^{3-}-P concentration, NH_4^+-N -N concentration, organic carbon (SOC) concentration, active and exchangeable pH, and soil texture by study site for the full seven-year study.

Variable	Site 1		Site 2		Site 3		Site 4	
	Mean (SD)	Range	Mean (SD)	Range	Mean (SD)	Range	Mean (SD)	Range
CO_2 flux (μmol CO_2 /m^2/s)	1.67 (0.52)	0.79, 2.73	1.29 (0.44)	0.37, 2.08	1.14 (0.58)	0.41, 2.33	1.32 (0.41)	0.74, 2.13
Soil Temperature (°C)	5.34 (2.33)	−0.14, 11.70	7.74 (2.71)	3.70, 18.45	8.32 (2.82)	2.00, 15.35	7.32 (2.20)	2.65, 11.65
Soil Moisture (%)	49.05 (24.91)	6.43, 100.00	14.70 (9.80)	3.25, 38.23	16.75 (10.45)	3.10, 39.25	23.20 (10.62)	4.25, 53.58
PO_4^{3-}-P (μg PO_4^{3-}-P/ g soil)	4.00 (3.16)	1.00, 16.30	2.81 (3.36)	0.03, 16.93	3.34 (1.48)	0.88, 5.85	3.37 (2.38)	0.18, 10.10
NH_4^+-N (μg NH_4^+-N/ g soil)	20.65 (8.53)	4.40, 36.18	10.92 (5.07)	3.59, 24.72	14.31 (7.95)	4.88, 31.04	17.87 (6.68)	8.91, 33.13
SOC (μg C/ g soil)	12.07 (2.76)	5.18, 15.09	4.65 (0.97)	3.12, 6.81	11.51 (2.19)	8.31, 15.16	9.29 (2.46)	5.31, 12.56
pH Active	4.85 (0.21)	4.11, 5.08	5.08 (0.47)	3.96, 6.77	5.48 (0.49)	4.33, 6.18	4.91 (0.45)	3.51, 5.39
pH Exchangeable	3.61 (0.12)	3.41, 3.94	3.79 (0.09)	3.64, 3.97	4.40 (0.40)	3.73, 5.02	3.75 (0.19)	3.30, 4.00
Texture (% sand)	58.40 (5.27)	66.59, 49.25	71.27 (3.87)	77.01, 61.72	50.23 (7.81)	72.48, 41.59	54.44 (2.83)	62.08, 50.15
Texture (% silt)	29.89 (5.14)	38.99, 20.33	19.73 (2.98)	30.60, 14.67	37.56 (8.31)	48.83, 22.08	33.58 (2.06)	37.29, 29.92
Texture (% clay)	11.71 (1.64)	13.76, 7.76	9.00 (1.59)	12.76, 7.00	12.21 (2.82)	7.76, 2.82	11.98 (1.55)	14.36, 8.00
Texture Classification	sandy loam		sandy loam		loam		sandy loam	

Table 3
Results of multiple regression model fitting with CO_2 flux (soil respiration) as the response variable. For each categorical variable in a model, regression *F* test results (*F* statistic and *p*-value) are reported. For each term involving a numerical variable, the estimated regression coefficient and regression *t*-test p-value are reported. A blank cell indicates the term was not included in that model. Bold font indicates the term was found to be a significant predictor of CO_2 flux at the 0.05 significance level. The four lowest-AIC models, which are also the highest (pseudo) R-squared ones, are indicated by asterisks.

Model	Model Terms								R^2, AIC
	Categorical (*F*, p-value)			Numerical (coefficient, p-value)					
	Site	Month	Year	Temp	Moist	$Temp^2$	$Moist^2$	Temp:Moist	
M1	12.71,	28.96,	14.80,						0.77,
	0.0000	**0.0000**	**0.0000**						114.7
M2	13.26,	20.42,	16.53,	0.035,					0.83,
	0.0000	**0.0000**	**0.0000**	**0.0128**					86.6
M3	1.55,	24.07,	8.78,		0.007,				0.83,
	0.2060	**0.0000**	**0.0000**		**0.0037**				92.9
M4	2.25,	16.83,	9.15,	0.043,	0.009,				0.90,
	0.0886	**0.0000**	**0.0000**	**0.0043**	**0.0031**				63.6
M5	14.69,	18.46,	16.71,	0.040,		−0.004,			0.85,
	0.0000	**0.0000**	**0.0000**	**0.0048**		**0.0469**			84.1
M6	1.11,	24.08,	7.49,		0.009,		−0.000,		0.83,
	0.3495	**0.0000**	**0.0000**		**0.0144**		0.4323		94.2
M7*	2.15,	12.55,	9.15,	0.052,	0.011,	−0.007,			0.94,
	0.0999	**0.0000**	**0.0000**	**0.0004**	**0.0002**	**0.0038**			55.5
M8	1.71,	17.02,	6.98,	0.044,	0.012,		−0.000,		0.91,
	0.1705	**0.0000**	**0.0000**	**0.0036**	**0.0066**		0.2760		64.1
M9	2.09,	16.29,	8.26,	0.042,	0.010,			0.000,	0.91,
	0.1082	**0.0000**	**0.0000**	**0.0045**	**0.0030**			0.3804	64.6
M10*	1.88,	12.50,	7.37,	0.052,	0.013,	−0.007,	−0.000,		0.94,
	0.1385	**0.0000**	**0.0000**	**0.0004**	**0.0030**	**0.0064**	0.5479		57.1
M11*	2.20,	12.11,	9.16,	0.054,	0.010,	−0.008,		−0.001,	0.94,
	0.0941	**0.0000**	**0.0000**	**0.0003**	**0.0022**	**0.0043**		0.4172	56.7
M12	1.72,	16.36,	6.92,	0.043,	0.012,		−0.000,	0.000	0.91,
	0.1695	**0.0000**	**0.0000**	**0.0040**	**0.0075**		0.4769	0.7598	66.0
M13*	1.73,	12.02,	7.26,	0.057,	0.014,	−0.009,	−0.000,	−0.001,	0.95,
	0.1674	**0.0000**	**0.0000**	**0.0002**	**0.0018**	**0.0023**	0.1904	0.1565	56.6

R^2 = Pseudo R-squared value of Nagerleke; AIC = Akaike Information Criterion.

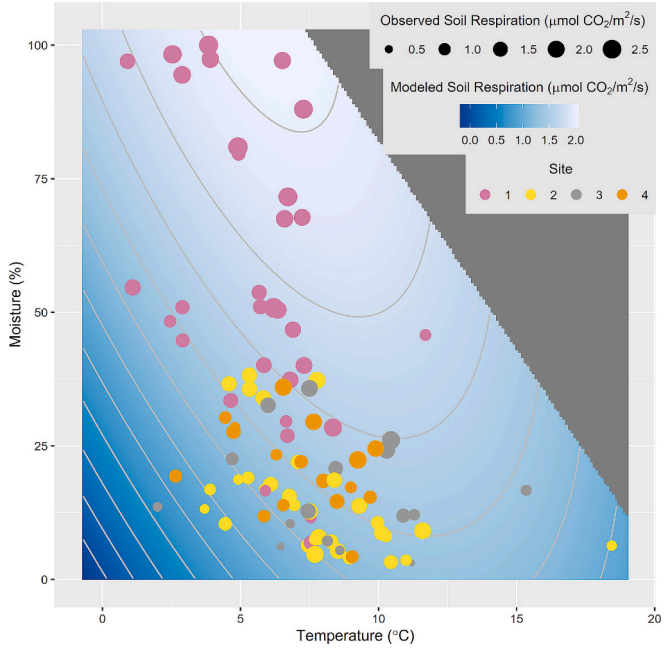


Fig. 2. Contour plot showing the full multiple regression model (3) (M13 in Table 3) fitted response surface, with soil respiration (CO_2 flux) as the response variable. Locations of points in the plot indicate the observed soil temperature and soil moisture values, their sizes indicate the observed CO_2 flux values, and their colors indicate sites at which the observations were made. There were no observations in the upper right section of the plot.

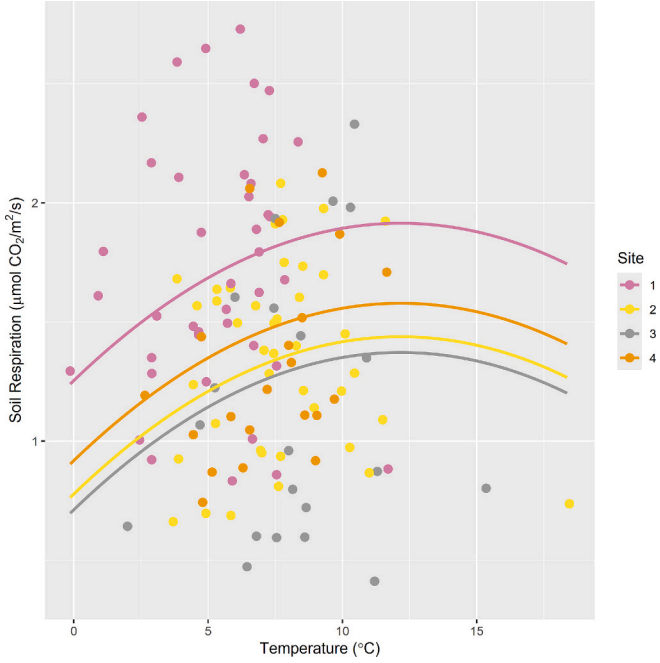


Fig. 3. Plot of observed CO_2 flux values (soil respiration) versus soil temperature, with fitted quadratic curve (M5 in Table 3) by site. Colors indicate sites at which the observations were made.

conditions had limited soil respiration. In this study, however, we found that soil respiration was elevated in the wet meadow site which had the highest levels of soil moisture (Fig. 4). During the growing season, soil was saturated 1–2 months each year in this site. This timeframe might be

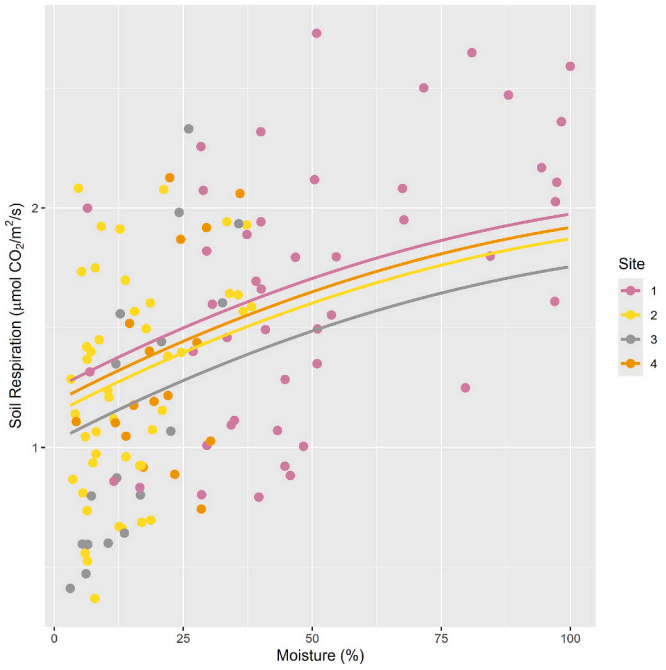


Fig. 4. Plot of observed CO_2 flux (soil respiration) values versus soil moisture, with fitted quadratic curve (M6 in Table 3) by site. Colors indicate sites at which the observations were made.

short enough to limit the formation of truly anoxic conditions. In addition, others found that soil respiration was suppressed at high soil moisture concentrations in soils with high clay content (Moyano et al., 2012; Xu et al., 2016). The soil in site 1 was a sandy loam and thus, did not have a particularly high clay content (Table 2).

The lower rates of soil respiration recorded at high soil temperatures could possibly be explained by an interaction between soil temperature and soil moisture. The highest soil temperatures were recorded in areas with low soil moisture (Fig. 2), which is known to suppress soil respiration (Liu et al., 2009; Orchard and Cook, 1983; Smith, 2005). Indeed, we found that models that incorporated the interaction between soil temperature and soil moisture (M11 and M13 in Table 3) explained the data equally well compared to those that did not incorporate the interaction term (M7 and M10 in Table 3). Averaged across all sites and years, soil temperature was highest in August and lowest in June. This relationship is the opposite of soil moisture which was highest in June and lowest in August. It appears that soil temperature and soil moisture may influence soil respiration, with each playing a more important role at different times through the summer.

Soil moisture in this system is strongly dependent on snowmelt and it generally peaks with melting snow in early summer (Harpold and Molotch, 2015; Jay et al., 2023). The sites were clear of snow in mid-June except in 2019 when the area experienced an above-average snowpack (Natural Resource Conservation Service, 2019) and snow remained in sites 1 and 4 until July.

These results suggest that with a changing climate, soil respiration may increase with warming, but the overall increase may be limited by decreased soil moisture (Liu et al., 2009; Orchard and Cook, 1983; Smith, 2005) and in some cases, abnormally high soil temperatures (Carey et al., 2016; Pietikainen et al., 2005). Our geospatial analysis indicates that in Rocky Mountain National Park, the average annual maximum air temperature will increase through the end of the century (Fig. 5). However, the average annual snowfall will decrease (Fig. 6) and the number of snow-free days will increase (Fig. 7). Consequently, we also noted a decrease in annual soil moisture (Fig. 8). From these modeling results and our field data, it appears that with a changing climate, SOC losses due to increased heterotopic soil respiration may be limited. While soil temperatures will become more favorable for microbial decomposition, soil moisture availability, especially in mid to late summer, may suppress microbial activity for much of the snow-free period.

Texture (% sand and % clay) were significantly related to CO_2 flux. Percent clay was positively related to CO_2 flux and percent sand was negatively related. This result may be related to the effect of the soil's

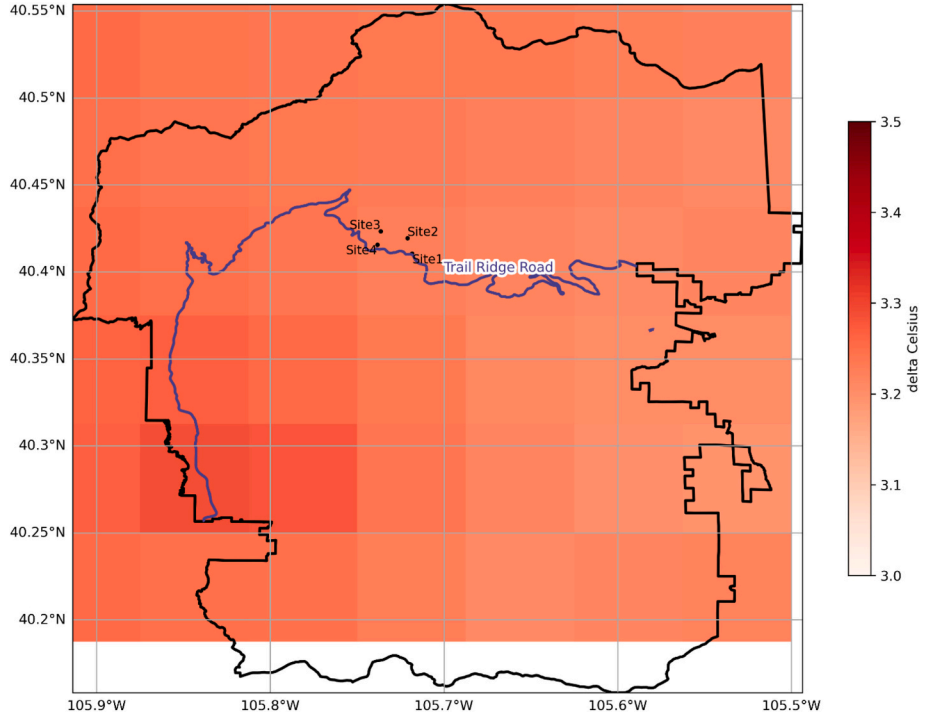


Fig. 5. Average Annual Difference in Daily Maximum Air Temperature between 1950 and 1999 and 2090–2099 for Rocky Mountain National Park in degrees Celsius. All areas of RMNP are expected to increase at least 3 degrees Celsius (Abatzoglou, 2014).

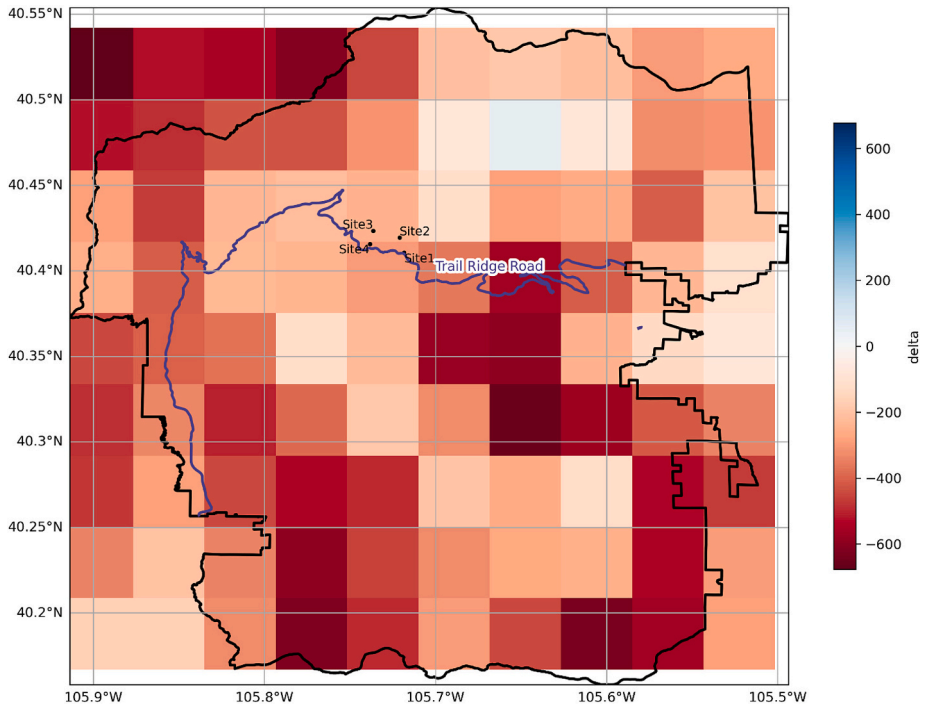


Fig. 6. Average Annual Difference in Snowfall (mm) between 1950 and 1999 and 2090–2099 for Rocky Mountain National Park. Most areas will see a decrease in snowfall (Alder and Hostetler, 2021).

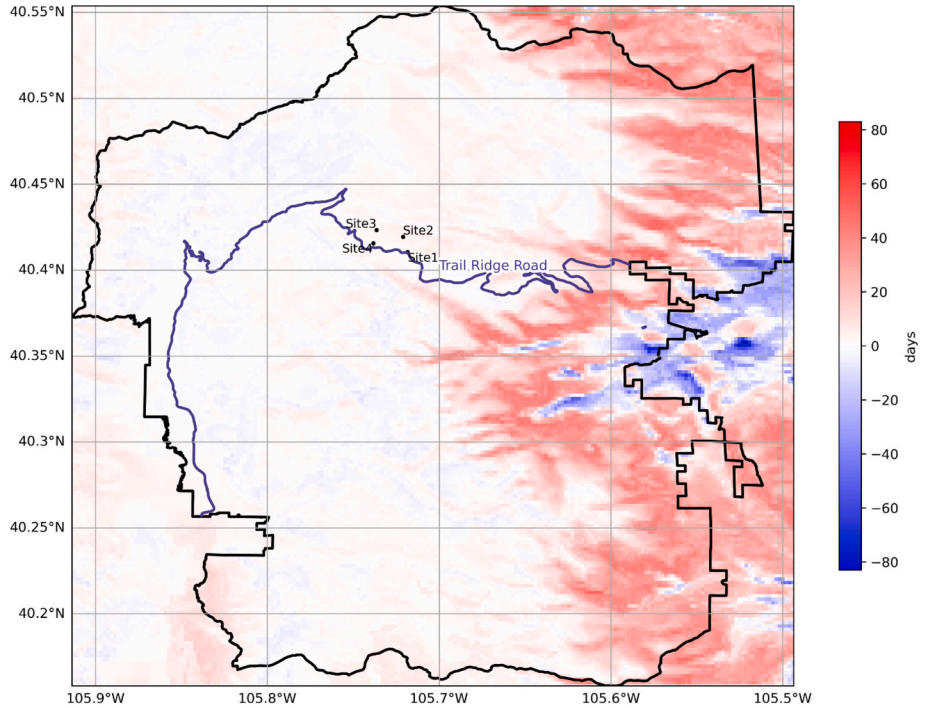


Fig. 7. Change in Annual Snow-Free Days for Rocky Mountain National Park during the period 2071–2100 compared to pre-climate change estimates using CMIP5. Areas in red indicate more snow-free days, while areas in blue represent fewer snow-free days (Abatzoglou et al., 2022).

nutrient and water holding capacity, with clay enhancing these parameters and sand decreasing them. Soils with greater nutrients and soil water are likely more favorable to microbes which in turn would result in higher CO_2 flux from these soils (Geering and So, 2017).

In this study, NH_4^+-N, PO_4^{3-}-P, active pH, and exchangeable pH were not significantly correlated with soil respiration. While these parameters have been shown to influence microbial growth and heterotrophic soil respiration, many of these studies were conducted in laboratory settings with very controlled environments (Craine et al., 2007; Giesler et al., 2012; Guo et al., 2022; Xu et al., 2016). It may be that in a natural setting, soil temperature and soil moisture more strongly influence respiration than the relatively subtle influence of nutrients or pH.

Across the seven years of this study, we did not detect a significant change in SOC. This result may indicate that SOC is not being lost at a

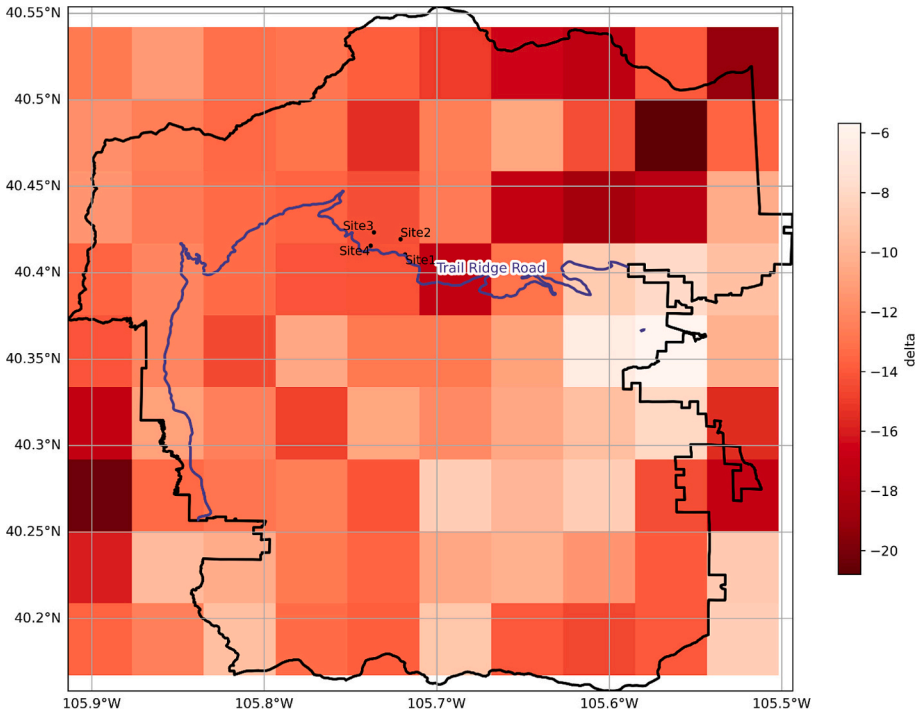


Fig. 8. Average Annual Difference in Soil Water Storage (%) between 1950 and 1999 and 2090–2099 for Rocky Mountain National Park. All areas in the park will experience a decrease in soil moisture (Alder and Hostetler, 2021).

rapid rate from this system, although seven years is a reasonably short period of time. Compared to SOC levels measured in the Southern Rocky Mountain tundra by Retzler in 1974 (2.79–17.22 %) and Birkeland et al. in 1987 (0.12–13.34 %), the levels of SOC we found in this study (0.15–30.9 %) ranged slightly higher. However, 93 % of the samples fell within the range found by Retzler and Birkland et al. (0.012–17.22 %). The samples in this study with SOC above 17.22 % were rare, found in only 7 % of samples, but were recorded in all 4 sites at least once (Table 2). Taken together, these results seem to suggest that SOC may be reasonably stable in this system, at least at this time.

5. Conclusion

From our data, it appears that SOC may be more stable than expected in some alpine tundra systems. In high alpine areas in Rocky Mountain National Park, climate modeling indicates that by the end of the century, the area is expected to become hotter and drier, especially in late summer. Our data indicate that soil respiration may be limited under low soil moisture conditions and high soil temperature. These soil conditions likely limit microbial growth and activity which in turn may limit SOC loss. Our data also appear to show that in natural systems, SOC decomposition and C loss are driven most strongly by soil temperature and soil moisture. Other parameters including soil nutrients and pH may play a role in soil respiration, but in our system, it appears that their impact is swamped by the overwhelming influence of soil temperature and soil moisture.

CRediT authorship contribution statement

Sarah A. Schliemann: Writing – review & editing, Writing – original draft, Visualization, Validation, Supervision, Resources, Project administration, Methodology, Investigation, Funding acquisition, Formal analysis, Data curation, Conceptualization. **Nels Grevstad:** Writing – review & editing, Writing – original draft, Visualization, Validation, Software, Methodology, Formal analysis, Data curation. **David A. Parr:** Writing – review & editing, Writing – original draft, Visualization, Validation, Software, Methodology, Investigation, Formal analysis, Data curation.

Funding

This project was funded in part by a grant from the National Parks Service (United States Department of the Interior) agreement number P18AC00622.

Declaration of competing interest

The authors declare the following financial interests/personal relationships which may be considered as potential competing interests: financial support was provided by National Parks Service (United States Department of the Interior).

Acknowledgements

The authors would like to thank the many, many MSU Denver undergraduate students who participated in all aspects of this paper.

Data availability

Data will be made available upon request.

References

Abatzoglou, J.T., 2014. Multivariate Adaptive Constructed Analogs (MACA) Statistical Downscaling Method CONUS [Dataset]. http://tds-proxy.nkn.uidaho.edu/thredds/nw.csc.climate-macav2livneh.aggregated.html.

Abatzoglou, J., Lute, A., Link, T., 2022. SnowClim v1.0: High-resolution Snow Model and Data for the wesTern United States [Dataset]. https://doi.org/10.6071/M3WM3G.

Agilent, 2025. Accessed 2025. https://www.agilent.com/.

Alder, J.R., Hostetler, S.W., 2021. CMIP5 MACAv2-METDATA Monthly Water Balance Model Projections 1950–2099 for the Contiguous United States: U.S. Geological Survey Data Release [dataset]. https://doi.org/10.5066/P9B2O22V.

Almazroui, M., Islam, M.N., Saeed, F., Saeed, S., Ismail, M., Ehsan, M.A., Diallo, I., O'Brien, E., Ashfaq, M., Martinez-Castro, D., Cavazos, T., Cerezo-Mota, R., Tippett, M.K., Gutowski, W.J., Alfaro, E.J., Hidalgo, H.G., Vichot-Llano, A., Campbell, J.D., Kamil, S., Rashid, I.U., Sylla, M.B., Stephenson, T., Taylor, M.,

Barlow, M., 2021. Projected changes in temperature and precipitation over the United States, Central America, and the Caribbean in CMIP6 GCMs. Earth Syst. Environ. 5 (1), 1–24.
Alster, C.J., Robinson, J.M., Arcus, V.L., Schipper, L.A., 2022. Assessing thermal acclimation of soil microbial respiration using macromolecular rate theory. Biogeochemistry 158 (1), 131–141.
Auer, I., Bohm, R., Jurkovic, A., Lipa, W., Orlik, A., Potzmann, R., Schoner, W., Ungersbock, M., Matulla, C., Briffa, K., Jones, P., Efthymiadis, D., Brunetti, M., Nanni, T., Maugeri, M., Mercalli, L., Mestre, O., Moisselin, J.M., Begert, M., Muller-Westermeier, G., Kveton, V., Bochnicek, O., Stastny, P., Lapin, M., Szalai, S., Szentimrey, T., Cegnar, T., Dolinar, M., Gajic-Capka, M., Zaninovic, K., Majstorovic, Z., Nieplova, E., 2007. HISTALP – historical instrumental climatological surface time series of the greater alpine region. Int. J. Climatol. 27 (1), 17–46.
Birkeland, P.W., Burke, R.M., Shroba, R.R., Geological, S., 1987. Holocene Alpine Soils in Gneissic Cirque Deposits, Colorado Front Range, 1590-E.;ch. E. Department of the Interior, U.S. Geological Survey, Reston, VA.
Bockheim, J.G., Munroe, J.S., 2014. Organic carbon pools and genesis of alpine soils with permafrost: a review. Arct. Antarct. Alp. Res. 46 (4), 987–1006.
Burnham, K., Anderson, D. (Eds.), 2002. Model Selection and Multimodel Inference: A Practical Information-Theoretic Approach. Springer, New York.
Campbell Scientific, 2025. Accessed 2025. https://www.campbellsci.com/.
Carey, J.C., Tang, J.W., Templer, P.H., Kroeger, K.D., Crowther, T.W., Burton, A.J., Dukes, J.S., Emmett, B., Frey, S.D., Heskel, M.A., Jiang, L., Machmuller, M.B., Mohan, J., Panetta, A.M., Reich, P.B., Reinsch, S., Wang, X., Allison, S.D., Bamminger, C., Bridgham, S., Collins, S.L., De Dato, G., Eddy, W.C., Enquist, B.J., Estiarte, M., Harte, J., Henderson, A., Johnson, B.R., Larsen, K.S., Luo, Y., Marhan, S., Melillo, J.M., Peuelas, J., Pfeifer-Meister, L., Poll, C., Rastetter, E., Reinmann, A.B., Reynolds, L.L., Schmidt, I.K., Shaver, G.R., Strong, A.L., Suseela, V., Tietema, A., 2016. Temperature response of soil respiration largely unaltered with experimental warming. Proc. Natl. Acad. Sci. USA 113 (48), 13797–13802.
Craine, J.M., Morrow, C., Fierer, N., 2007. Microbial nitrogen limitation increases decomposition. Ecology 88 (8), 2105–2113.
Davidson, E.A., Janssens, I.A., 2006. Temperature sensitivity of soil carbon decomposition and feedbacks to climate change. Nature 440 (7081), 165–173.
Davidson, E.A., Belk, E., Boone, R.D., 1998. Soil water content and temperature as independent or confounded factors controlling soil respiration in a temperate mixed hardwood forest. Glob. Chang. Biol. 4 (2), 217–227.
Dethier, D.P., Williams, N., Fields, J.F., 2022. Snowmelt-driven seasonal infiltration and flow in the upper critical zone, Niwot ridge (Colorado), USA. Water 14 (15), 17.
Dong, Z., Driscoll, C.T., Campbell, J.L., Pourmokhtarian, A., Stoner, A.M.K., Hayhoe, K., 2019. Projections of water, carbon, and nitrogen dynamics under future climate change in an alpine tundra ecosystem in the southern Rocky Mountains using a biogeochemical model. Sci. Total Environ. 650, 1451–1464.
Fassnacht, S.R., Venable, N.B.H., McGrath, D., Patterson, G.G., 2018. Sub-seasonal snowpack trends in the Rocky Mountain National Park Area, Colorado, USA. Water 10 (5), 19.
Friedlingstein, P., O'Sullivan, M., Jones, M.W., Andrew, R.M., Gregor, L., Hauck, J., Le Quéré, C., Luijkx, I.T., Olsen, A., Peters, G.P., Peters, W., Pongratz, J., Schwingshackl, C., Sitch, S., Canadell, J.G., Ciais, P., Jackson, R.B., Alin, S.R., Alkama, R., Arneth, A., Arora, V.K., Bates, N.R., Becker, M., Bellouin, N., Bittig, H.C., Bopp, L., Chevallier, F., Chini, L.P., Cronin, M., Evans, W., Falk, S., Feely, R.A., Gasser, T., Gehlen, M., Gkritzalis, T., Gloege, L., Grassi, G., Gruber, N., Gürses, Ö., Harris, I., Hefner, M., Houghton, R.A., Hurtt, G.C., Iida, Y., Ilyina, T., Jain, A.K., Jersild, A., Kadono, K., Kato, E., Kennedy, D., Klein Goldewijk, K., Knauer, J., Korsbakken, J.I., Landschützer, P., Lefèvre, N., Lindsay, K., Liu, J., Liu, Z., Marland, G., Mayot, N., McGrath, M.J., Metzl, N., Monacci, N.M., Munro, D.R., Nakaoka, S.I., Niwa, Y., O'Brien, K., Ono, T., Palmer, P.I., Pan, N., Pierrot, D., Pocock, K., Poulter, B., Resplandy, L., Robertson, E., Rödenbeck, C., Rodriguez, C., Rosan, T.M., Schwinger, J., Séférian, R., Shutler, J.D., Skjelvan, I., Steinhoff, T., Sun, Q., Sutton, A.J., Sweeney, C., Takao, S., Tanhua, T., Tans, P.P., Tian, X., Tian, H., Tilbrook, B., Tsujino, H., Tubiello, F., van der Werf, G.R., Walker, A.P., Wanninkhof, R., Whitehead, C., Willstrand Wranne, A., Wright, R., Yuan, W., Yue, C., Yue, X., Zaehle, S., Zeng, J., Zheng, B., 2022. Global carbon budget 2022. Earth Syst. Sci. Data 14 (11), 4811–4900.
Gee, G.W., Bauder, J.W., 1986. Particle size analysis. In: Klute, A. (Ed.), Methods of Soil Analysis: Part 1 Physical and Mineralogical Methods [1]. Soil Science Society of America, Madison, WI.
Geering, H.R., So, H.B., 2017. Texture; Book Chapter Thesis, pp. 2323–2329.
Giesler, R., Esberg, C., Lagerstrom, A., Graae, B.J., 2012. Phosphorus availability and microbial respiration across different tundra vegetation types. Biogeochemistry 108 (1–3), 429–445.
Gruber, S., 2012. Derivation and analysis of a high-resolution estimate of global permafrost zonation. Cryosphere 6 (1), 221–233.
Guo, M., Zhao, B., Wen, Y.X., Hu, J.J., Dou, A.M., Zhang, Z.W., Rui, J.P., Li, W.J., Wang, Q., Zhu, J.X., 2022. Elevational pattern of soil organic carbon release in a Tibetan alpine grassland: consequence of quality but not quantity of initial soil organic carbon. Geoderma 428, 11.
Gutiérrez, J.M., Jones, R.G., Narisma, G.T., Alves, L.M., Amjad, M., Gorodetskaya, I.V., Grose, M., Klutse, N.A.B., Krakovska, S., Li, J., Martínez-Castro, D., Mearns, L.O., Mernild, S.H., Ngo-Duc, T., Hurk, B.V.D., Yoon, J.-H., 2021. Atlas. In: Masson-Delmotte, P.Z.V., Pirani, A., Connors, S.L., Péan, C., Berger, S., Caud, N., Chen, Y., Goldfarb, L., Gomis, M.I., Huang, M., Leitzell, K., Lonnoy, E., Matthews, J.B.R., Maycock, T.K., Waterfield, T., Yelekçi, O., Yu, R., Zhou, B. (Eds.), Climate Change 2021: The Physical Science Basis. Contribution of Working Group I to the Sixth Assessment Report of the Intergovernmental Panel on Climate Change. Cambridge University Press, Cambridge and New York, pp. 1927–2058.
Hach CO, 2025. Accessed 2025. https://www.hach.com/.
Harpold, A.A., Molotch, N.P., 2015. Sensitivity of soil water availability to changing snowmelt timing in the western US. Geophys. Res. Lett. 42 (19), 8011–8020.
Janke, J.R., 2005. The occurrence of alpine permafrost in the front range of Colorado. Geomorphology 67 (3–4), 375–389.
Janssens, I.A., Dieleman, W., Luyssaert, S., Subke, J.A., Reichstein, M., Ceulemans, R., Ciais, P., Dolman, A.J., Grace, J., Matteucci, G., Papale, D., Piao, S.L., Schulze, E.D., Tang, J., Law, B.E., 2010. Reduction of forest soil respiration in response to nitrogen deposition. Nat. Geosci. 3 (5), 315–322.
Jay, K.R., Wieder, W.R., Swenson, S.C., Knowles, J.F., Elmendorf, S.C., Holland-Moritz, H., Suding, K.N., 2023. Topographic heterogeneity and aspect moderate exposure to climate change across an alpine tundra hillslope. J. Geophys. Res. Biogeosci. 128 (11), 20.
Kemmitt, S.J., Wright, D., Goulding, K.W.T., Jones, D.L., 2006. pH regulation of carbon and nitrogen dynamics in two agricultural soils. Soil Biol. Biochem. 38 (5), 898–911.
Knowles, J.F., Blanken, P.D., Williams, M.W., 2015. Soil respiration variability across a soil moisture and vegetation community gradient within a snow-scoured alpine meadow. Biogeochemistry 125 (2), 185–202.
Knowles, J.F., Blanken, P.D., Lawrence, C.R., Williams, M.W., 2019. Evidence for non-steady-state carbon emissions from snow-scoured alpine tundra. Nat. Commun. 10, 9.
Kutner, M., Nachtsheim, C., Neter, J., 2004. Applied Linear Regression Models, 4 ed. McGraw-Hill/Irwin.
IPCC, 2023: Summary for policymakers. In: Lee, H., Romero, J. (Eds.), 2023. Climate Change 2023: Synthesis Report. Contribution of Working Groups I, II and III to the Sixth Assessment Report of the Intergovernmental Panel on Climate Change. IPCC, Geneva, Switzerland.
Leifeld, J., Zimmermann, M., Fuhrer, J., 2008. Simulating decomposition of labile soil organic carbon: effects of pH. Soil Biol. Biochem. 40 (12), 2948–2951.
Li-Cor, 2025. Accessed 2025. https://www.licor.com/.
Liu, W.X., Zhang, Z., Wan, S.Q., 2009. Predominant role of water in regulating soil and microbial respiration and their responses to climate change in a semiarid grassland. Glob. Chang. Biol. 15 (1), 184–195.
Liu, J.P., Zhao, Y.Y., Yang, Y., Xu, S.H., Zhang, F.H., Zhang, X.L., Shi, L.H., Qiu, A.G., 2017. A mixed geographically and temporally weighted regression: exploring spatial-temporal variations from global and local perspectives. Entropy 19 (2), 20.
Liu, Y., He, N.P., Wen, X.F., Xu, L., Sun, X.M., Yu, G.R., Liang, L.Y., Schipper, L.A., 2018. The optimum temperature of soil microbial respiration: patterns and controls. Soil Biol. Biochem. 121, 35–42.
Lloyd, J., Taylor, J.A., 1994. On the temperature-dependence of soil respiration. Funct. Ecol. 8 (3), 315–323.
Mahony, C.R., Wang, T.L., Hamann, A., Cannon, A.J., 2022. A global climate model ensemble for downscaled monthly climate normals over North America. Int. J. Climatol. 42 (11), 5871–5891.
Minder, J.R., Letcher, T.W., Liu, C., 2018. The character and causes of elevation-dependent warming in high-resolution simulations of Rocky Mountain climate change. J. Clim. 31 (6), 2093–2113.
Moyano, F.E., Vasilyeva, N., Bouckaert, L., Cook, F., Craine, J., Yuste, J.C., Don, A., Epron, D., Formanek, P., Franzluebbers, A., Ilstedt, U., Katterer, T., Orchard, V., Reichstein, M., Rey, A., Ruamps, L., Subke, J.A., Thomsen, I.K., Chenu, C., 2012. The moisture response of soil heterotrophic respiration: interaction with soil properties. Biogeosciences 9 (3), 1173–1182.
Moyano, F.E., Manzoni, S., Chenu, C., 2013. Responses of soil heterotrophic respiration to moisture availability: an exploration of processes and models. Soil Biol. Biochem. 59, 72–85.
Natural Resource Conservation Service, 2019. Colorado Water Supply Outlook Report June 1, 2019.
Orchard, V.A., Cook, F.J., 1983. Relationship between soil respiration and soil-moisture. Soil Biol. Biochem. 15 (4), 447–453.
Pepin, N., Bradley, R.S., Diaz, H.F., Baraer, M., Caceres, E.B., Forsythe, N., Fowler, H., Greenwood, G., Hashmi, M.Z., Liu, X.D., Miller, J.R., Ning, L., Ohmura, A., Palazzi, E., Rangwala, I., Schoner, W., Severskiy, I., Shahgedanova, M., Wang, M.B., Williamson, S.N., Yang, D.Q., Mountain Research Initiative, E.D.W.W.G, 2015. Elevation-dependent warming in mountain regions of the world. Nat. Clim. Chang. 5 (5), 424–430.
Pietikainen, J., Pettersson, M., Baath, E., 2005. Comparison of temperature effects on soil respiration and bacterial and fungal growth rates. FEMS Microbiol. Ecol. 52 (1), 49–58.
Pinheiro, J., Bates, D., DebRoy, S., Sarkar, D., R Core Team, 2025. Accessed nlme: Linear and Nonlinear Mixed Effects Models. R package version 3.1–140. https://CRAN.R-project.org/package=nlme.
Rasmussen, R., Ikeda, K., Liu, C.H., Gochis, D., Clark, M., Dai, A.G., Gutmann, E., Dudhia, J., Chen, F., Barlage, M., Yates, D., Zhang, G., 2014. Climate change impacts on the water balance of the Colorado headwaters: high-resolution regional climate model simulations. J. Hydrometeorol. 15 (3), 1091–1116.
Ren, F., Yang, X.X., Zhou, H.K., Zhu, W.Y., Zhang, Z.H., Chen, L.T., Cao, G.M., He, J.S., 2016. Contrasting effects of nitrogen and phosphorus addition on soil respiration in an alpine grassland on the Qinghai-Tibetan plateau. Sci. Rep. 6, 10.
Retzer, J.L., 1974. Alpine soils. In: Ives, J.D., Barry, R.G. (Eds.), Arctic and Alpine Environments. Routledge, Abingdon, Oxon, pp. 771–802.
Rousk, J., Brookes, P.C., Baath, E., 2009. Contrasting soil pH effects on fungal and bacterial growth suggest functional redundancy in carbon mineralization. Appl. Environ. Microbiol. 75 (6), 1589–1596.
Schuur, E.A.G., Bockheim, J., Canadell, J.G., Euskirchen, E., Field, C.B., Goryachkin, S. V., Hagemann, S., Kuhry, P., Lafleur, P.M., Lee, H., Mazhitova, G., Nelson, F.E., Rinke, A., Romanovsky, V.E., Shiklomanov, N., Tarnocai, C., Venevsky, S., Vogel, J.

G., Zimov, S.A., 2008. Vulnerability of permafrost carbon to climate change: implications for the global carbon cycle. Bioscience 58 (8), 701–714.
Shahbaz, M., Bengtson, P., Mertes, J.R., Kulessa, B., Kljun, N., 2022. Spatial heterogeneity of soil carbon exchanges and their drivers in a boreal forest. Sci. Total Environ. 831, 13.
Shimadzu, 2025. Accessed 2025. https://www.shimadzu.com/.
Sigma Aldrich, 2025. Accessed 2025. https://www.sigmaaldrich.com/US/en.
Sims, G.K., Ellsworth, T.R., Mulvaney, R.L., 1995. Microscale determination of inorganic nitrogen in water and soil extracts. Commun. Soil Sci. Plant Anal. 26 (1–2), 303–316.
Smith, V.R., 2005. Moisture, carbon and inorganic nutrient controls of soil respiration at a sub-Antarctic Island. Soil Biol. Biochem. 37 (1), 81–91.
Soil Survey Staff, Accessed, 2025. Web Soil Survey. https://websoilsurvey.sc.egov.usda.gov/app/.
Song, J., Wan, S., Piao, S., Knapp, A.K., Classen, A.T., Vicca, S., Ciais, P., Hovenden, M.J., Leuzinger, S., Beier, C., Kardol, P., Xia, J.Y., Liu, Q., Ru, J.Y., Zhou, Z.X., Luo, Y.Q., Guo, D.L., Langley, J.A., Zscheischler, J., Dukes, J.S., Tang, J.W., Chen, J.Q., Hofmockel, K.S., Kueppers, L.M., Rustad, L., Liu, L.L., Smith, M.D., Templer, P.H., Thomas, R.Q., Norby, R.J., Phillips, R.P., Niu, S.L., Fatichi, S., Wang, Y.P., Shao, P.S., Han, H.Y., Wang, D.D., Lei, L.J., Wang, J.L., Li, X.N., Zhang, Q., Li, X.M., Su, F.L., Liu, B., Yang, F., Ma, G.G., Li, G.Y., Liu, Y.C., Liu, Y.Z., Yang, Z.L., Zhang, K.S., Miao, Y., Hu, M.J., Yan, C., Zhang, A., Zhong, M.X., Hui, Y., Li, Y., Zheng, M.M., 2019. A meta-analysis of 1,119 manipulative experiments on terrestrial carbon-cycling responses to global change. Nat. Ecol. Evol. 3 (9), 1309–1320.
Sun, S.B., Che, T., Gentine, P., Chen, Q.T., Wang, L.C., Yan, Z.F., Chen, B.Z., Song, Z.L., 2021. Shallow groundwater inhibits soil respiration and favors carbon uptake in a wet alpine meadow ecosystem. Agric. For. Meteorol. 297.
Tebaldi, C., Debeire, K., Eyring, V., Fischer, E., Fyfe, J., Friedlingstein, P., Knutti, R., Lowe, J., O'Neill, B., Sanderson, B., van Vuuren, D., Riahi, K., Meinshausen, M., Nicholls, Z., Tokarska, K.B., Hurtt, G., Kriegler, E., Lamarque, J.F., Meehl, G., Moss, R., Bauer, S.E., Boucher, O., Brovkin, V., Byun, Y.H., Dix, M., Gualdi, S., Guo, H., John, J.G., Kharin, S., Kim, Y., Koshiro, T., Ma, L.B., Olivie, D., Panickal, S., Qiao, F.L., Rong, X.Y., Rosenbloom, N., Schupfner, M., Seferian, R., Sellar, A., Semmler, T., Shi, X.Y., Song, Z.Y., Steger, C., Stouffer, R., Swart, N., Tachiiri, K., Tang, Q., Tatebe, H., Voldoire, A., Volodin, E., Wyser, K., Xin, X.G., Yang, S.T., Yu, Y. Q., Ziehn, T., 2021. Climate model projections from the scenario model intercomparison project (ScenarioMIP) of CMIP6. Earth Syst. Dynam. 12 (1), 253–293.
Thomas Scientific, 2025. Accessed. https://www.thomassci.com/.
Treseder, K.K., 2008. Nitrogen additions and microbial biomass: a meta-analysis of ecosystem studies. Ecol. Lett. 11 (10), 1111–1120.
Turetsky, M.R., Abbott, B.W., Jones, M.C., Anthony, K.W., Olefeldt, D., Schuur, E.A.G., Grosse, G., Kuhry, P., Hugelius, G., Koven, C., Lawrence, D.M., Gibson, C., Sannel, A. B.K., McGuire, A.D., 2020. Carbon release through abrupt permafrost thaw. Nat. Geosci. 13 (2), 138-+.
Wardle, D.A., 1992. A comparative-assessment of factors which influence microbial biomass carbon and nitrogen levels in soil. Biol. Rev. 67 (3), 321–358.
Wikle, C.K., Zammit-Mangion, A., Cressie, N., 2019. Spatio-Temporal Statistics with R. Chapman & Hall/CRC, Boca Raton, FL.
Wu, M.H., Chen, S.Y., Chen, J.W., Xue, K., Chen, S.L., Wang, X.M., Chen, T., Kang, S.C., Rui, J.P., Thies, J.E., Bardgett, R.D., Wang, Y.F., 2021. Reduced microbial stability in the active layer is associated with carbon loss under alpine permafrost degradation. Proc. Natl. Acad. Sci. USA 118 (25), 9.
Xu, X., Shi, Z., Li, D.J., Rey, A., Ruan, H.H., Craine, J.M., Liang, J.Y., Zhou, J.Z., Luo, Y. Q., 2016. Soil properties control decomposition of soil organic carbon: results from data-assimilation analysis. Geoderma 262, 235–242.
Xue, K., Yuan, M.M., Shi, Z.J., Qin, Y.J., Deng, Y., Cheng, L., Wu, L.Y., He, Z.L., Van Nostrand, J.D., Bracho, R., Natali, S., Schuur, E.A.G., Luo, C.W., Konstantinidis, K.T., Wang, Q., Cole, J.R., Tiedje, J.M., Luo, Y.Q., Zhou, J.Z., 2016. Tundra soil carbon is vulnerable to rapid microbial decomposition under climate warming. Nat. Clim. Chang. 6 (6), 595-+.
Zhou, Y.M., Meng, G.L., Tai, Z.J., Han, J.Q., Deng, J.F., Wang, H.W., Li, M.H., 2019. Effects of experimental warming on growing season temperature and carbon exchange in an alpine tundra ecosystem. Russ. J. Ecol. 50 (5), 474–481.